Journal of Peptide Science, Vol. 3, 299–313 (1997)

Structural Comparison in Solution of a Native and Retro Peptide Derived From the Third Helix of *Staphylococcus aureus* Protein A, Domain B: Retro Peptides, a Useful Tool for the Discrimination of Helix Stabilization Factors Dependent on the Peptide Chain Orientation

THOMAS HAACK, YOLANDA M. SÁNCHEZ, MARÍA-JOSÉ GONZÁLEZ and ERNEST GIRALT

Department of Organic Chemistry, University of Barcelona, Barcelona, Spain

Received 6 January 1997
Accepted 24 March 1997

Abstract: A peptide fragment corresponding to the third helix of *Staphylococcus Aureus* protein A, domain B, was chosen to study the effect of the main-chain direction upon secondary structure formation and stability, applying the retro-enantio concept. For this purpose, two peptides consisting of the native (Ln) and reversed (Lr) sequences were synthesized and their conformational preferences analysed by CD and NMR spectroscopy. A combination of CD and NMR data, such as molar ellipcitity, NOE connectivities, Hα and NH chemical shifts, $^3J_{\alpha N}$ coupling constants and amide temperature coefficients indicated the presence of nascent helices for both Ln and Lr in water, stabilized upon addition of the fluorinated solvents TFE and HFIP. Helix formation and stabilization appeared to be very similar in both normal and retro peptides, despite the unfavourable charge–macrodipole interactions and bad N-capping in the retro peptide. Thus, these helix stabilization factors are not a secondary structure as determined for this specific peptide. In general, the synthesis and confirmational analysis of peptide pairs with opposite main-chain directions, normal and retro peptides, could be useful in the determination of secondary structure stabilization factors dependent on the direction.

J. Pep. Sci. 3: 299–313
No. of Figures: 8. No. of Tables: 2. No. of Refs: 39

Keywords: NMR; retro-enantio; helix; macrodipole; protein A

INTRODUCTION

Over the past few years, the use of peptides with inverted chirality (enantiopeptides) has received much attention on account of their greater stability against degradation by proteases, probably the most severe limitation to the use of normal peptides as therapeutic agents. The so-called 'retro-enantio' concept [1–3] is especially attractive in that it combines the use of D-amino acids (for the formation of enantiopeptides) with a reversal of the 'direction' of the peptide chain backbone (retro-peptides). This reversal simply involves constructing a new peptide in which, if the native sequence has '*i*' amino acids, amino acid '*i*' is placed at position 1 of the new peptide, amino acid '*i*–1' at position 2 and so on until amino acid 1 of the native peptide occupies position '*i*' of the retro peptide. If the retro-enantio concept is applied to the construction of new peptides based on the sequence of a native bioactive peptide, the result is a peptide that combines inversion of configuration at the α carbon atoms of the constituent amino acids with the reversal of the direction of the peptide backbone. The overall effect

Abbreviations: ACN, acetonitrile; R_t, *retention time; SpA DB: Staphylococcus aureus Protein A fragment B.*

Correspondence: Ernest Giralt, Department of Organic Chemistry, University of Barcelona, Martí I Franqués 1-11, 08028 Barcelona, Spain. Tel +34 3 4021262; fax: +34 3 3397878, e-mail: giralt@mafalda.qui.ub.es

CCC 1075-2617/97/040299-15

is to create a peptide having the same topological distribution as the native one but at the same time having a strongly enhanced stability to proteases.

The generality of the retro-enantio concept has recently been questioned [4, 5] Although the concept is probably valid for small peptides with a large degree of flexibility, it is doubtful that it can be applied in the cases of larger molecules having pronounced conformation preferences. The key to the in-depth study of this question is the detailed investigation of the changes in conformation brought about by application of the retro-enantio concept to peptide molecules. Assuming that the systematic inversion of configuration of the constituent amino acids (except Ile and Thr) of a peptide molecule leads simply to enantiomeric confirmations, the comparison of the conformation of peptides and their corresponding retro-sequences becomes the key issue.

Apart from its interest in attempting to define the scope of the retro-enantio concept, the conformational analysis of peptides and retro-peptides is also relevant in other areas. The conformation of peptide molecules in general and, more specifically, their tendency to adopt a given secondary structure such as α-helices or β-sheets, is determined by two sets of factors: (1) the amino acids that make up the sequence and (2) the relative order of these amino acids (review for helices [6]). Concerning point (1), it is well known that certain amino acids statistically favour the adoption of certain secondary structures. In point (2) various factors such as electrostatic interaction between charges, dipole interactions and so on come into play. However, the contribution that each of these considerations makes to the overall three-dimensional structure is not clear cut. It is obvious, nonetheless, that a given peptide in its 'wild' and 'retro' versions are indistinguishable with regard to their amino acid compositions; (point (1) above). In this paper, the usefulness of the comparative conformational analysis of normal and retro peptides for the study of the factors that stabilize secondary structures, without interference from differences in amino acid composition between peptides, are discussed for the first time.

As a model to investigate the effect of backbone orientation on helical conformation and stability, we have used the peptide segment 38–59 of the domain B (DB) of *Staphyloccocus aureas* protein A (SpA). SpA is known to be a virtually universal immunoglobulin (IgG) binding protein. X-ray crystallography of the complex, SpA–IgG fragment Fc, showed two antiparallel helices formed by the N-terminal part, but a low electron density in the C-terminal part (residues 38–59) attributed to peptide flexibility or structural disorder [7]. Nevertheless, solution studies of the isolated domain B [8] showed a well-defined, three helix bundle with a hydrophobic core formed by the apolar faces of the slightly amphiphilic helices, helix I 9–19, helix II 26–37 and helix III 42–55 (Figure 1). Helix III is flanked by two prolines, which serve as helix start and stop signals. Furthermore, the N-terminal Pro preceding residue is Asp38, known to be a good N-capping residue and able to interact favourably with the partially positively charged N-terminus (charge–macrodipole interaction). In addition, the C-terminal Pro following the Lys residue interacts favourably with the macrodipole at the carboxy terminus. In consequence, helix III from Asp38 to Lys59 in isolation was expected to form a helix in solution. Reverting this sequence results in unfavourable charge–macro dipole interactions of the amino (Lys) and carboxy (Asp) residues and a poor N-cap residue (Lys). These unfavourable interactions should give, in principle, a lower helical content for the retro peptide compared with the normal peptide, if these factors are important for helix stabilization. In the present work, we present the synthesis and conformational analysis by CD and high field NMR of SpA DB 38–59 in its native and retro forms and study the effect of sequence reversal on helix stabilization.

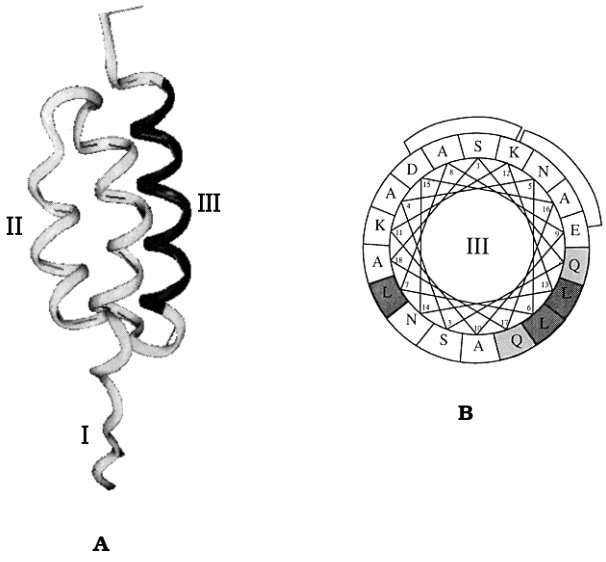

Figure 1 (A: Solution structure of *Staphylococcus aureus* protein A, domain B. Only the peptide backbone is shown. Helices I and II are shown in light grey, helix III in dark grey. (B) Primary sequence of helix III and its representation in the helical wheel.

MATERIALS AND METHODS

Peptide Synthesis and Purification

The native (Ln) and retro (Lr) peptides, sequence 38–59 of *Staphylococcal* protein A domain B, were synthesized automatically on an Applied Biosystem, model 430A, according to the standard Boc strategy for solid-phase synthesis using a 'small-scale rapid cycle' (SSRC) protocol. For trifunctional amino acids the following derivatives were used: Boc-Lys(CI-Z)OH), Boc-Ser(Bzl)OH, Boc-Asp(cHex)OH, Boc-Glu(cHex)OH. The peptides were assembled on a *p*-MBHA resin (loading = 0.81 mmol/g resin) using a single symmetrical anhydride coupling step with 10 eq. of Boc-protected amino acids and 5 eq. coupling reagents (DCC, HOBt). After capping the liberated amino termini with a mixture of acetic anhydride/pyridine (1:1), the peptides were cleaved from the resin and simultaneously deprotected by single step acidolysis with anhydrous HF and anisole as scavenger, yielding the C-terminal peptide amides. Crude peptide products were precipitated with diethyl ether, centrifuged or filtered, dissolved in 10% aqueous acetic acid and lyophilized. Peptides were purified to homogeneity (> 95%) by reversed-phase (Vydac C18) medium pressure liquid chromatography; (RP-MPLC), applying an increasing amount of ACN/H_2O (0.05% TFA) as eluent. Purity was determined by RP-HPLC (Nucleosil C18, linear gradient 5% ACN to 65% ACN (0.036% TFA) in 20 min, flow rate 1 ml/min; R_t(Ln) = 11.4 min; R_t(Lr) = 12.0 min) and capillary zone electrophoresis (CZE). The purified peptides were characterized by amino acid analysis and mass spectrometry (electrospray and MALDI) prior to the NMR experiments.

Circular Dichroism

Circular dichroism spectra were recorded on a JASCO-720 spectrometer controlled by a standard PC computer equipped with the JASCO software package J-700. Optical cells with a path length of 0.1 cm were placed in a thermostable cell holder and temperature was regulated by a thermostat, model Neslab, with an accuracy of 0.3°C. The concentration of the peptides were in the range of 80 μM, as determined by quantitative amino acid analysis, and they were dissolved in 3 mM potassium phosphate buffer containing 15 mM KF at pH 5. The effect of cosolvent titration was determined for TFE from 0% to 100% in 15% steps and, additionally, for 18% HFIP. Temperature dependence was measured for all solvent systems from 278 K to 348 K. Three scans between 190 and 260 nm in a step size of 0.1 nm, were recorded and an average value of the three scans taken.

CD was expressed as mean residue ellipticities $[\Theta]_m$ in deg $cm^2/dmol^{-1}$, which is related to the molar elipticity $\Delta\varepsilon$ by $[\Theta]_m = (3298 \times \Delta\varepsilon)/N$, where N is the number of residues.

NMR Spectroscopy

Samples were prepared using a concentration of 2 mM peptide in 600 μl containing 150 mM phosphate buffer and 0.01 mM NAN_3 dissolved either in (A) 85% H_2O/15% D_2O, (B) 65% H_2O/25% d_2-hexafluoroisopropanol (HFIP)/10% D_2O or (C) 50% H_2O/50% *d*3-trifluoroethanol (RFE). Ph was adjusted to 5.2 using small aliquots of 0.1N sodium hydroxide or phospheric acid. Dioxane was used as internal standard.

^{1}H-NMR spectra were recorded on a Varian VXR-500 unit equipped with a shielded triple resonance gradient unit. A 90 degree pulse was generated applying a 12.4 μs pulse at a transmitter power of 56 dB and the transmitter on-resonance on the H_2O signal. 2D-homonuclear NMR spectra were recorded in phase-sensitive mode using the States method for quadrature detection in the *t*l dimension. DQF-COSY [9] and clean-TOCSY [10] were recorded with a MLEV-17 spin-lock sequence [11] at a mixing time of 80 ms, and NOESY [12,13] were recorded with mixing times of 100 s, 200 s and 400 ms to evaluate spin-diffusion effects. Mixing times were varied randomly by 10% to avoid zero-quantum effects. ROESY [14] spectra were acquired at low mixing times (80–120 ms) to differentiate between ROE connectives and chemical exchange peaks. Solvent suppression was achieved for TOCSY and NOESY/ROESY using a WATERGATE sequence [15] and presaturation of 1.5 s for the DQF-COSY. The acquisition time for two-dimensional spectra was in general set to 0.2 s, followed by a recovery delay of 1.6 s. A spectral width of 5000 Hz was used in both dimensions containing 2048 to 1024 data points. Usually 24 to 32 scans for 256 increments were recorded to achieve sufficient resolution. Spectra were processed with the Varian built in software package VNMR on a SUN-SPARC work station. Zero-filling or linear prediction of the *t*1 dimension results in a matrix of 2 × 4 K, which was baseline corrected in both *F*1 and *F*2 dimensions and multiplied by either a shifted Gaussian or sine-bell function prior to the Fourier transform.

Approximate $^{3}J_{NH-H\alpha}$ coupling constants were measured after analysing the corresponding 1D slices from resolution enhanced DQF-COSY spectra with a 4 × 1 K real data-point matrix. Temperature coefficients of the amide protons were extracted from high resolution 1D or fast-TOCSY (256 increments containing eight transients with 2048 data points each) in 5 K intervals from 278 K to 308 K.

RESULTS

Circular Dichroism of Fragment 38–59 (Ln) and its Retro Analogue (Lr)

The far-UV CD spectra of both Ln and Lr peptides (Figure 2 in aqueous solution at pH = 5.3 exhibited a strong minimum at 200 nm, accompanied by a small shoulder at 222 nm, characteristic for largely disordered conformations with residual or nascent helices. Upon addition of the structure-stabilizing cosolvents TFE or HFIP [16–18], a stronger absorption was observed for the minimum at 222 nm, a maximum emerged at 190 nm and the minimum above 200 nm exhibited a shift to higher wavelengths. Additionally, both minima at 222 and 200 nm increased in intensity with increasing TFE concentration. Thus, the resulting CD spectra at 50% TFE or 18% HFIP reflect the characteristics of an α-helix with the typical minima at 208 and 222 nm, accompanied by a maximum at 198 nm ([19] and references cited therein). The occurrence of an isodichroic point at 203 nm for both Ln and Lr is compatible with a two-state conformational equilibrium between unordered and helical structures. The concentration dependence (between 0.08 and 1.0 mM) of the minimum at 222 nm was linear (data not shown), excluding aggregation phenomena, often observed for hydrophobic or amphipathic peptides such as the present one. Thermal denaturation studies (data not shown) showed a linear decrease in ellipticity at 222 nm with increasing temperature, consistent with a cooperative transition between the folded and the unfolded state. The recovery of ellipticity by recooling to 278 K indicated the reversibility of the folding process and allowed irreversible thermal denaturation to be excluded.

In water, the calculated helicity (using %helicity = 100 × [Θ_{222}/−39,500 deg cm^2/dmol × (1 − 2.57/n)], n = 22 number of peptide bonds [20]) for the native peptide Ln was higher than for the retro peptide Lr (Ln 25%; Lr 12%). In contrast, a maximum of ≈60% helicity was reached for both Ln and Lr upon addition of 50% TFE or 18% HFIP. Thus, CD results suggest structural similarities in the presence of cosolvents but differences in the absence of cosolvents.

NMR

Association or aggregation phenomena as a reason for secondary structure formation can be excluded both from NMR and CD concentration dependency

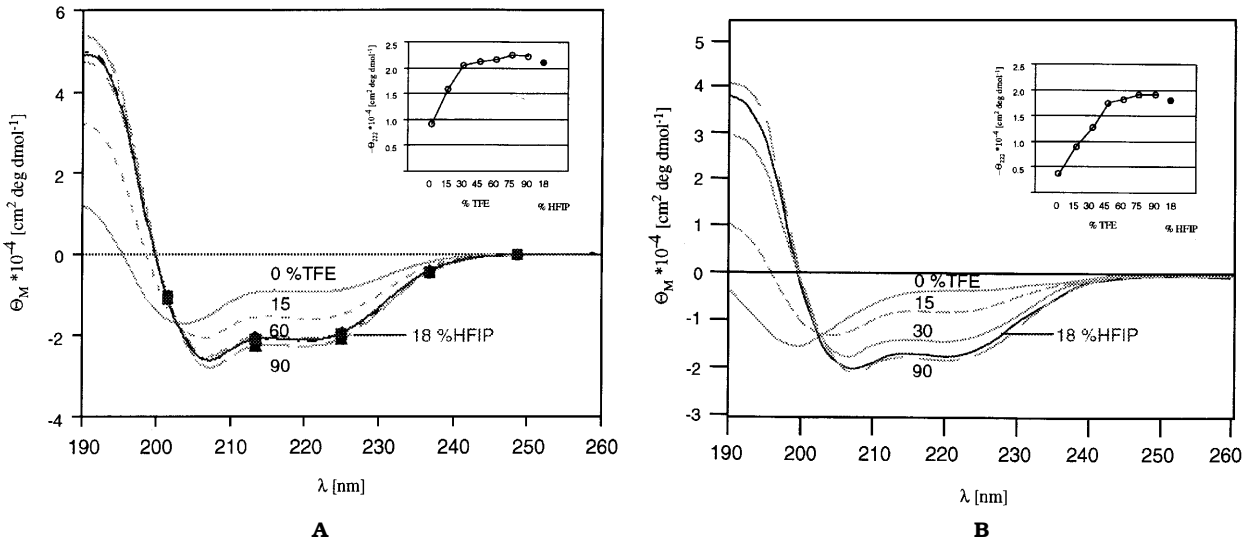

Figure 2 CD spectra of the cosolvent titration of Ln (A) and Lr (B) at 5°C. The TFE and HFIP percentages (by vol.) used were the following: 0%, 15%, 30%, 45%, 60%, 75%, 90%, 18% HFIP. Insets represent the molar ellipticity at 222 nm of the cosolvents titration for Ln (open bars) and Lr (closed bars).

studies. As mentioned above, CD spectra of Ln and Lr in the concentration range of 80 μM to 1 mM did not change in the absence and presence of cosolvents. NMR showed the absence of amide line broadening or of significant changes in the chemical shift at 3 mM concentration when compared with 0.3 mM concentration. Additional evidence for the presence of single monomeric species derived from the temperature dependency of the amide chemical shifts, which were linear between 5 and 30°C.

Assignments were done using the standard two-step procedure [21, 22] by a combination of 2D homonuclear through bond TOCSY and through space NOESY or ROESY experiments. Spin diffusion effects leading to three spin NOE connectivities were excluded by checking the presence of the same NOES observed at low mixing times in the NOESY or ROESY spectra.

NMR of the Native (Ln) and Retro (Lr) Peptide in Water

The ^{1}H-NMR spectra of both native and retro peptides in aqueous solution show a small chemical shift dispersion for both amide and H^α region, as typically observed for very flexible peptides (Figure 3). The assignment was complicated by the presence of slow *cis–trans* rotational isomerism about the Xaa-Pro tertiary amide bond. ROESY spectra were recorded to differentiate between chemical exchange peaks arising from slow *cis–trans* isomerism and pure ROESY cross-peaks, which occur in opposite phases. Nevertheless, the absence of amide chemical shift degeneration made the unambiguous assignment for the major, all-*trans* conformer, based upon the $\alpha N(i,i+1)$ connectivities possible (Tables 1 and 2). Additionally, a region of continuous but low-intensity $NN(i,i+1)$ and $\beta N(i,i+1)$ NOEs from Ala43 to Gin56 confirmed the prior assignment. The two Pro residues were assigned by their characteristic NOE connectivities $\alpha N(\text{Pro,Xaa}+1)$ and $\alpha\delta(\text{Xaa, Pro}+1)$ for the *trans* or $\alpha\alpha(\text{Xaa,Pro}+1)$ for the *cis* conformer.

The presence of continuous $NN(i,i+1)$ (Figur4A and B) and some $\alpha N(i,i+2)$ NOEs (Figure 4) suggest a nascent helix, defined as an ensemble of turns over a range of residues [23]. Long range and further medium range NOEs, as typically observed for highly ordered structures, were clearly absent.

Further evidence for nascent helices was derived from the small but significant upfield shift of the H^α protons when compared with 'random coil' values from Wishart ([25] and references cited herein). As shown in Figure 6, a succession of helix-specific negative values is observed throughout the sequence from Gln41 to Gln56. Additionally, a three to four residue periodicity of the H^α and NH (data not shown) chemical shift deviations for both Ln and Lr point to the presence of an amphiphilic helix. The strongest deviation from 'random coil' values were observed for the polar residues. Glu48, Asp54 and Asn53, and the lowest deviation for the apolar residues Leu46, Ala49 and Leu52. The interpretation of the alteration of the chemical shift deviation of the Pro adjacent residues Gln41, Ser42 and Gln56, Ala57, located on the apolar face of the schematic amphiphilic helical wheel (Figure 1), is not clear.

The use of other conformationally sensitive parameters such as amide temperature coefficients, helpful for identifying hydrogen bonds [26–29], or $^2J_{NH\alpha}$ coupling constants, which gives information about Φ dihedral angles ([30,31] and references cited there), has been reported in the literature to give additional support for the presence of nascent helices. In such case, amide temperature coefficients have been used to calculate solvent protection factors per residue (Pf), assuming a linear dependence between completely solvent-shielded (0 p.p.b./K) and completely solvent-exposed (values from [32]) amide protons. The native peptide Ln shows a mean solvent protection Pf of 55%, derived mainly from the 12 residues Leu45 to Gln56 with the exception of the two acidic residues Glu48 and Asp54. In contrast, in the case of the retro peptide Lr only eight residues from Leu45 to Leu52 (with the exception of Lys50) are involved in hydrogen bonds, giving a Pf of 44%. Thus, both Ln and Lr contain amide protons involved in hydrogen bonds in the central part of the molecules starting with Leu45, but differ in the relative stability and length of this hydrogen bonded array. The observed $^3J_{NH\alpha}$ coupling constants were in the range of 7 Hz. This value is in general attributed to non-ordered, flexible peptides, although recent statistical studies on the ϕ/Ψ distribution of helices in proteins contained in the Brookhaven database [33] show a range of possible; Φ-angles ($-45°$ to $-100°$) corresponding to $^3J_{NH\alpha}$ coupling constants between 3 and 9 Hz.

The results presented so far could provide a very demanding test for theoretical or semi-empirical secondary structure prediction algorithms. Such a comparison between the experimental (H^α chemical shifts) and calculated helicity was performed with the recently developed algorithm AGADIR [34–36]. AGADIR is based on the two-state helix–coil approx-

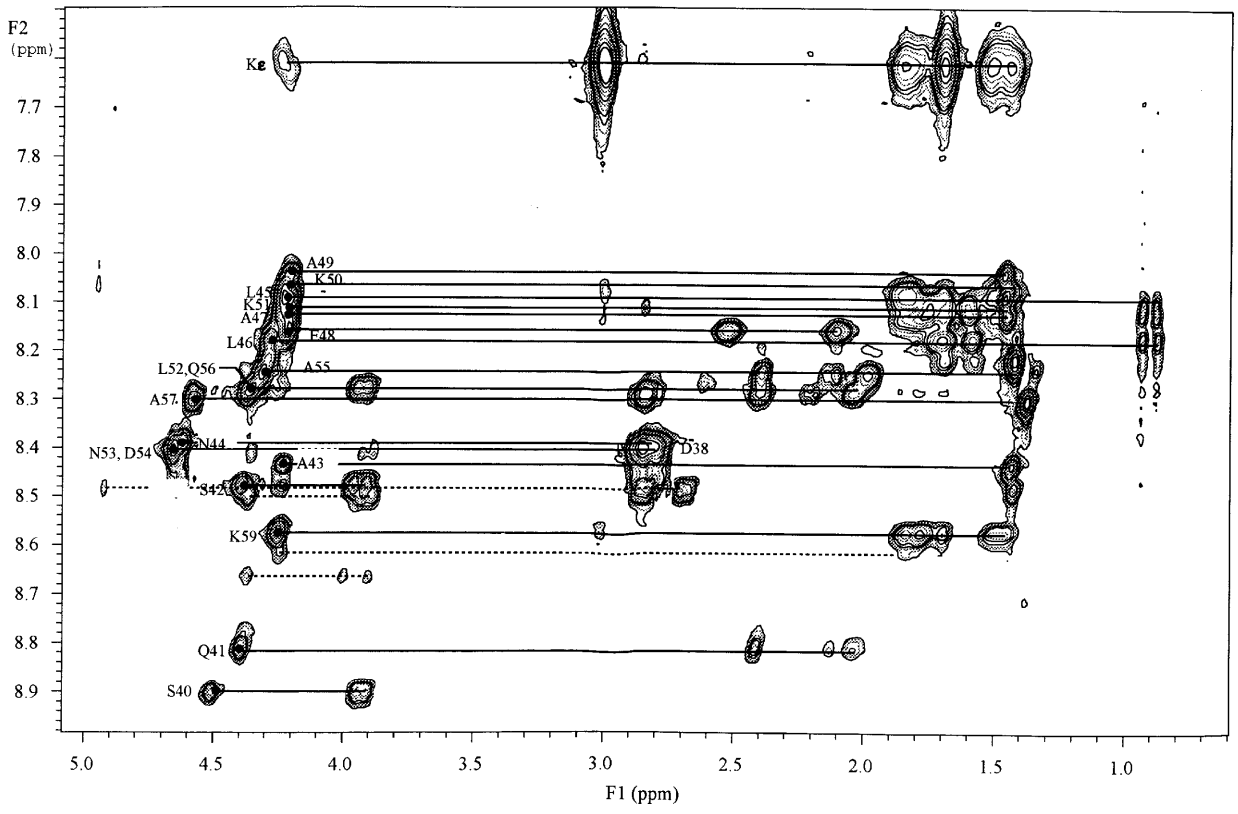

A

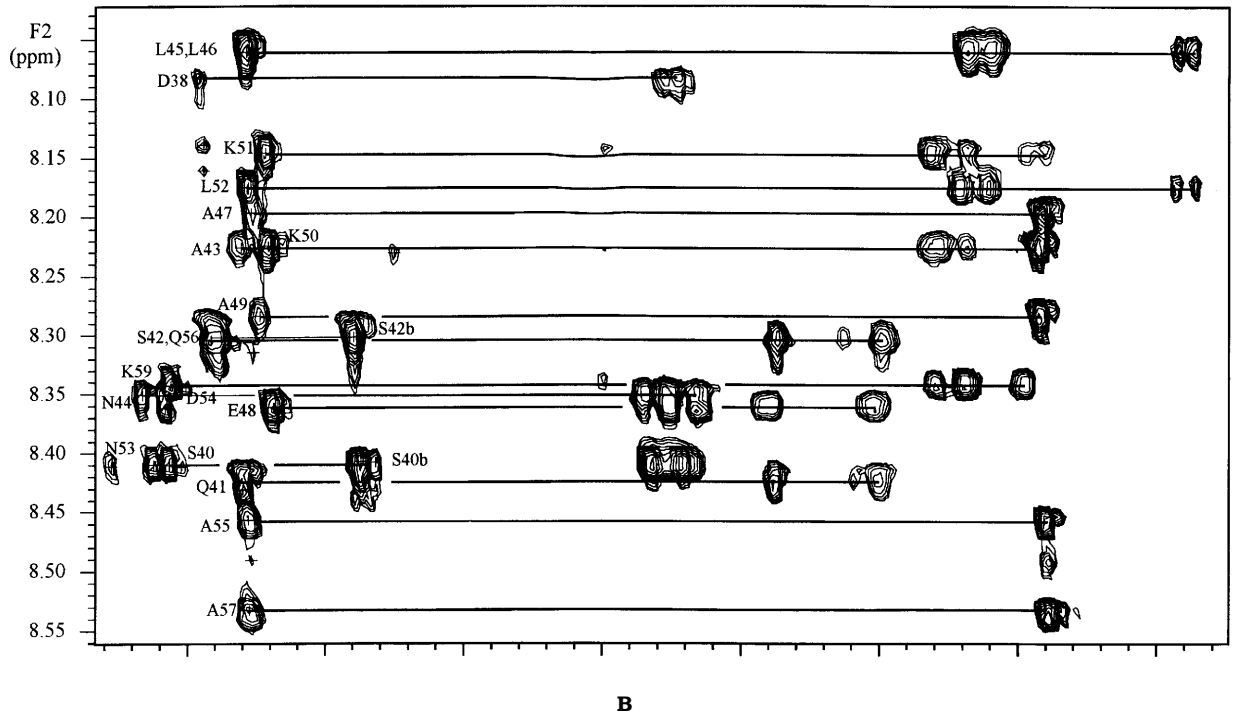

B

Figure 3 2D-homonuclear TOCSY, amide–alkyl zone of (A) Ln and (B) Lr in water. Ln at 10°C and Lr at 5°C. Spin system connectivities are indicated by continuous lines.

Table 1 Chemical Shifts (5°C) and Amide Temperature Coefficients ($\Delta NH/\Delta T$) of Ln in Water and 18% HFIP (*italic*) at pH = 5.2

Residue	NH	Hα	Hβ1	Hβ2	Hγ	Others		ΔNH/ΔT (p.p.b./K)
Asp 38	8.40	n.d.	2.85					7.8
	7.94	*4.99*	*2.87*	*2.78*				*5.6*
Pro 39		4.50	2.25	2.00	1.87	3.79	3.63	
		4.47	*2.34*	*2.05*	*2.08*	*3.92*		
Ser 40	8.91	4.51	3.94	3.92				5.8
	8.77	*4.57*	*4.05*	*3.96*				5.1
Gln 41	8.81	4.38	2.13	2.03	2.41			8.6
	8.92	*4.35*	*2.17*	*2.10*	*2.45*			7.5
Ser 42	8.48	4.39	3.95	3.91				5.1
	8.25	*4.32*	*3.94*					4.2
Ala 43	8.44	4.23	1.43					6.5
	8.12	*4.15*	*1.48*					2.6
Asn 44	8.38	4.60	2.84					5.1
	7.94	*4.52*	*2.87*					2.9
Leu 45	8.12	4.21	1.78		1.59	0.93	0.87	2.0
	7.86	*4.17*	*1.80*		*1.71*	*0.90*	*0.88*	3.2
Leu 46	8.18	4.28	1.70		1.58	0.93	0.87	2.6
	7.99	*4.10*	*1.77*	*1.68*	*1.61*	*0.87*		4.6
Ala 47	8.05	4.20	1.45					x
	7.91	*4.08*	*1.53*					x
Glu 48	8.15	4.21	2.10		2.52			6.2
	7.90	*4.15*	*2.20*		*2.54*			1.3
Ala 49	8.12	4.21	1.45					4.4
	8.59	*4.03*	*1.52*					4.5
Lys 50	8.10	4.22	1.83	1.75	1.45	1.65		3.2
	8.48	*3.98*	*1.96*	*1.74*	*1.58*	*1.46*	1.66	4.8
Lys 51	8.13	4.21	1.83		1.44	1.77		2.0
	7.83	*4.10*	*2.03*	*1.74*	*1.45*	*1.68*		0.4
Leu 52	8.22	4.31	1.69		1.57	0.93	0.87	3.1
	8.35	*4.14*	*1.82*		*1.74*	*0.91*	*0.86*	5.4
Asn 53	8.41	4.65	2.84					2.6
	8.41	*4.46*	*2.82*					5.9
Asp 54	8.41	4.65	2.84					4.5
	8.49	*4.57*	*2.98*	*2.90*				4.7
Ala 55	8.22	4.28	1.42					3.1
	7.99	*4.27*	*1.54*					1.1
Gln 56	8.25	4.31	2.11	1.98	2.39			4.1
	7.86	*4.33*	*2.22*	*2.08*	*2.50*	*2.45*		6.4
Ala 57	8.30	4.57	1.37					6.8
	7.91	*4.55*	*1.45*					2.7
Pro 58		4.50	2.25	2.00	1.97	3.85	3.85	
		4.47	*2.34*	*1.94*	*2.08*	*3.85*	*3.66*	
Lys 59	8.58	4.24	1.83	1.78	1.48	1.70		8.0
	8.34	*4.34*	*1.91*	*1.82*	*1.54*	*1.74*		*9.1*

imation of the classical Zimm–Brag theory and takes into account most of the sequence-dependent factors for helix stabilization. AGADIR has been successfully used in the prediction of total helicity, as well as helicity on a residue basis of a variety of molecules. Figure 6 represents, for both Ln and Lr, a comparison between calculated (AGADIR) and experimental helicities (from H^{α} chemical shifts). Calculation suggests a central helix from Gln41 to Ala56, in good agreement with the experimental results. Nevertheless, AGADIR predicted differences between Ln and Lr in both location of the helix

Table 2 Chemical Shifts (5°C) and Amide Temperature Coefficients ($\triangle$NH/$\triangle T$) of Lr in Water and 18% HFIP (*italic*) at pH = 5.2

Residue	NH	Hα	Hβ1	Hβ2	Hγ	Others			$\triangle$NH/$\triangle T$ (p.p.b./K)
Asp 38	8.83	4.46	2.78	2.73					5.8
	8.25	*4.69*	*2.83*	*2.78*					3.3
Pro 39		4.41	2.32	1.90	2.01	3.87	3.64		
		4.30	*2.38*	*1.94*	*2.13*	*2.04*	*3.61*	*3.85*	
Ser 40	8.41	4.57	3.88						6.3
	7.98	*4.83*	*4.06*	*3.99*					*1.1*
Gln 41	8.42	4.30	2.01	2.10	2.39				7.2
	7.72	*4.46*	*2.32*	*2.13*	*2.52*				*< 1.0*
Ser 42	8.30	4.42	3.90						4.7
	8.24	*4.36*	*4.07*						*4.4*
Ala 43	8.22	4.33	1.43						4.4
	7.70	*4.26*	*1.49*						*< 1.0*
Asn 44	8.35	4.67	2.85	2.78					5.0
	8.32	*4.49*	*2.96*	*2.82*					*4.3*
Leu 45	8.06	4.29	1.69		1.61		0.93	0.88	3.9
	8.79	*4.08*	*1.80*		*1.68*		*0.90*		*6.0*
Leu 46	8.06	4.29	1.69		1.61		0.93	0.88	3.5
	8.36	*4.16*	*1.93*		*1.61*		*0.91*		*5.4*
Ala 47	8.20	4.27	1.42						3.7
	8.07	*4.16*	*1.61*						2.5
Glu 48	8.35	4.20	2.02		2.39				4.8
	8.44	*3.94*	*2.79*	*2.64*	*2.40*	*2.182*			*4.4*
Ala 49	8.29	4.25	1.43						4.1
	8.19	*4.08*	*1.57*						*7.5*
Lys 50	8.23	4.22	1.80		1.69		1.43		6.7
	7.79	*4.08*	*2.00*	*1.90*	*1.70*		*1.40*		*2.1*
Lys 51	8.14	4.22	1.83		1.69		1.42		4.2
	8.05	*4.07*	*2.03*	*1.96*	*1.73*		*1.43*		4.1
Leu 52	8.17	4.28	1.72		1.61		0.94	0.87	4.8
	8.08	*4.22*	*1.85*		*1.74*		*0.96*	*0.91*	*3.2*
Asn 53	8.41	4.63	2.83	2.72					5.1
	7.96	*4.52*	*3.00*	*2.86*					*< 1.0*
Asp 54	8.35	4.59	2.78	2.67					5.5
	8.18	*4.46*	*2.85*	*2.79*					1.9
Ala 55	8.54	4.26	1.40						7.4
	8.16	*4.15*	*1.51*						4.3
Gln 56	8.30	4.39	2.13	2.00	2.38				4.1
	8.27	*4.23*	*2.22*		*2.45*				1.2
Ala 57	8.46	4.28	1.41						7.6
	8.43	*4.23*	*1.61*						*4.7*
Pro 58		4.47	2.30	2.00	2.02	3.78			
		4.51	*2.38*	*2.02*	*2.10*	*3.85*			
Lys 59	8.34	4.57	1.80		1.70		1.48		7.6
	7.82	*4.52*	*1.88*	*1.80*	*1.79*		*1.59*		5.6

(Ln = Ser40–Asn53; Lr = Ser42–Ala56) and total helical amount, calculated over the whole sequence (Ln = 7.4% vs. Lr = 4.0%). NMR showed, in contrast, only marginal differences between Ln and Lr and, for both a higher helicity at the C-terminus than at the N-terminus.

NMR of the Native Peptide and its Retro Analogue in Fluorinated Cosolvents

For both native and retro peptide, 18% HFIP was selected as solvent for examining the effect of cosolvent addition on a residue basis by NMR. This

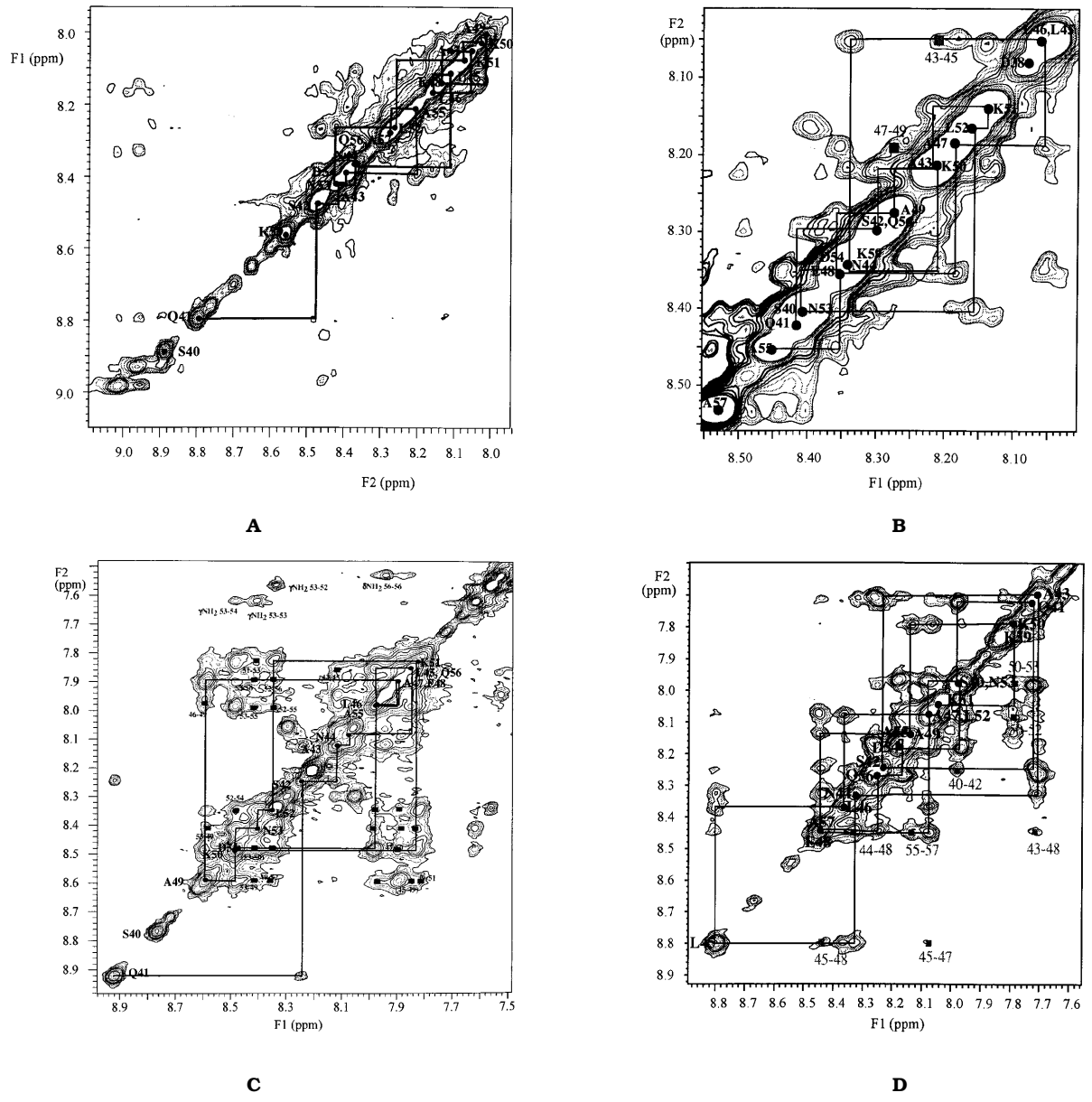

Figure 4 2D homonuclear NOESY, amide–amide zone of (A) Ln and (B) Lr in water and (C) Ln and (D) Lr in 18% HFIP (down level). Sequential assignment in the NOSEY spectrum is only given for the major conformer. Non-sequential medium range NOEs are indicated by squares with corresponding amino acid numbering.

solvent was shown from prior CD studies to stabilize the helical content significantly. The helix-stabilizing effect of 18% HFIP, both in Ln and Lr, is similar to the effect of 50% TFE. The differences between both physico chemically different solvent systems and their influence on the conformation on a residue basis by NMR have now been compared.

The presence of 18% HFIP did not change the amide of H^{α} chemical shift dispersion but did give a larger number of NOEs, thus facilitating in principle the assignment and secondary structure analysis. On the other hand, addition of this cosolvent provokes an increase in peak intensities of the second set of signals derived from *cis–trans* isomerization to nearly equal intensities. Nevertheless, unambiguous assignments for both sets of signals were made following the general procedure described above for aqueous solutions.

A high number of helix characteristic strong sequential NN ($i,i+1$) and medium range NN($i,i+3$),

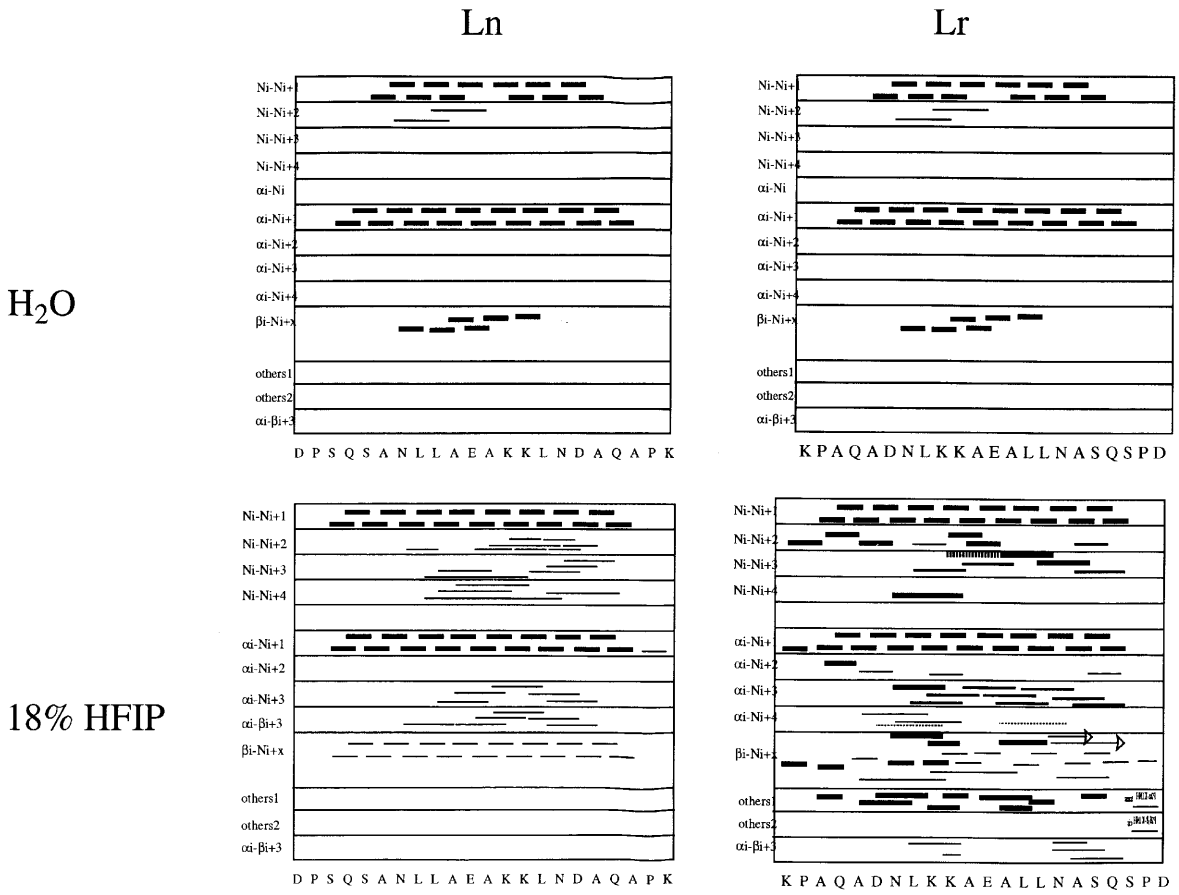

Figure 5 NOE summary for Ln (left panel) and Lr (right panel) in water (top panel) and 18% HFIP (bottom panel) at pH = 5.3. The heights of the bars indicate the relative intensities. Asterisks or broken lines indicate ambiguous connectivities owing to overlap.

$\alpha N(i,i+3)$, $\alpha\beta(i,i+3)$ NOEs were observed from Leu45 to Gln56 in the presence of 18% HFIP (Figure 4 C and D), which are consistent with stabilized helical conformations for both Ln and Lr. Ln show in 50% TFE similar NOE connectivities to those observed in 18% HFIP for the central region from (data not shown) Leu45 to Gln 56, but contain additional NOEs in the N-terminus, extending the helical segment from Ser40 to Gln56. Calculation of the total helical amount by the mean relative intensities of the sequential $NN(i,i+1)/\alpha N(i,i+1)$ NOEs [37] gives for Lr 55%, for Ln in 18% HFIP 60% and for Ln in 50% TFE 63%.

The presence of a stabilized helical conformation for the Ln and Lr was confirmed by a significant upfield shift of the H^{α} protons, compared with aqueous solution, as shown in Figure 7. Clearly four helical turns with a three to four residue periodicity were observed for Ln in the presence of 18% HFIP: Gln41–Leu45, Leu45–Glu48, Glu48–Leu52 and Leu52–Gln56. Thus, HFIP only stabilized the helix already presented in water and did not induce additional conformational features. Especially strong upfield shifts, in comparison with these observed in water, were observed in the second and third helical turn spanning the putative Glu48–Lys51 salt-bridge. The tendency of HFIP to stabilize the helix already present in water was even more marked for the retro peptide Lr. All residues in the helical segment showed an upfield shift of at least 0.15 p.p.m., with the exception of Leu52. No regular periodicity of three to four residues was observed for this peptide, pointing to a less amphipatic helical conformation. Furthermore, Glu48 changes from a local minimum (−0.16 p.p.m.) for Ln to a local maximum (−0.40 p.p.m.) for Lr, pointing to differences in the putative salt-bridge Glu48–Lys51. The comparison of the H^{α} chemical shift deviation between the two binary mixtures containing 50% TFE and 18% HFIP solvents was very interesting,

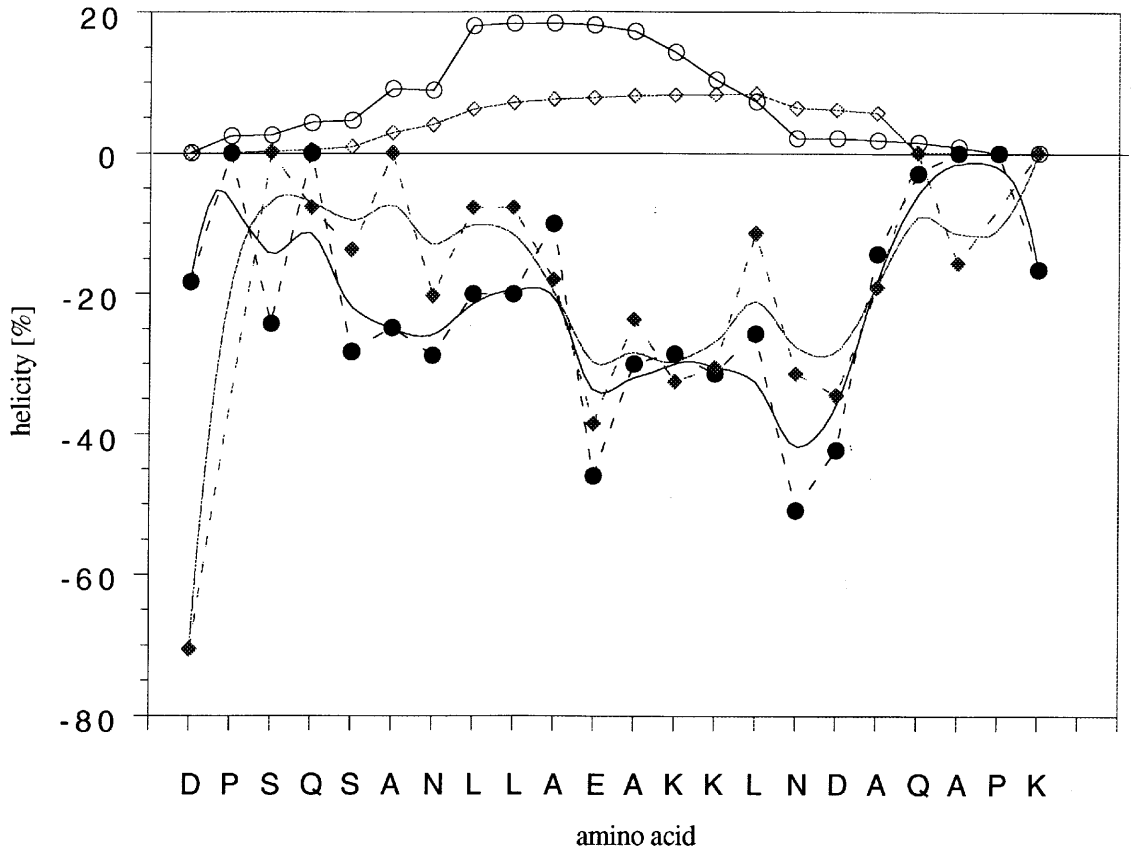

Figure 6 Comparison of the residue helicity of Ln and Lr based upon experimental H^{α} chemical shift deviation and calculations applying AGADIR as algorithm. Ln is represented by circles, Lr by squares. Calculated values are given in open symbols, experimental values in the inversed mode indicated by closed symbols. Experimental residue helicities are calculated supposing −0.38 p.p.m. as 100% helical.

showing a similar helical content by CD. As depicted in Figure 8, both solvent systems influence the secondary structure globally and locally on a residue basis in a very similar way, supporting the CD results. Finally, a good correlation of calculated helical content between CD and NMR data was found. The total helical contents of Ln and Lr were 37% (50% TFE and 18% HFIP) and 40% (18% HFIP), respectively, based upon the H^{α} conformational shifts using the equation $\%\text{helix} = \Sigma(\Delta\delta H^{\alpha})/(n \times -0.38)$, where −0.38 p.p.m. was taken to be the value for 100% helix and n, the number of amide bonds, is 22.

DISCUSSION

The present study was undertaken to examine the relationship between the effect of changes in the macrodipole direction and conformation. Furthermore, two known structure-stabilizing solvents, TFE and HFIP, were compared.

The model used in the present study derived from helix three, sequence 38–59, of *Staphylococcus aureus* protein A, domain B (SpA DB). This last helix consists of a slightly amphipathic helix (Figure 1), if one considers the amide side chain of Asn and Gln as hydrophobic residues. The hydrophobic face is slightly disturbed by the hydrophilic residue Ser42. The hydrophilic face contains two possible salt-bridges in $i+3$ spacing formed by Glu48–K51 and K51–Asp54. Calculation of the amphiphilic profile using different scales revealed two maxima at Leu45 and Leu52 and one minimum at Glu48 or Ala47, depending on the scale used. Two peptides representing the native (Ln) and the reversed or inverted sequence (Lr) of SpA DB (Figure 1) were synthesized and its conformational preferences analysed by a combined study of CD and NMR.

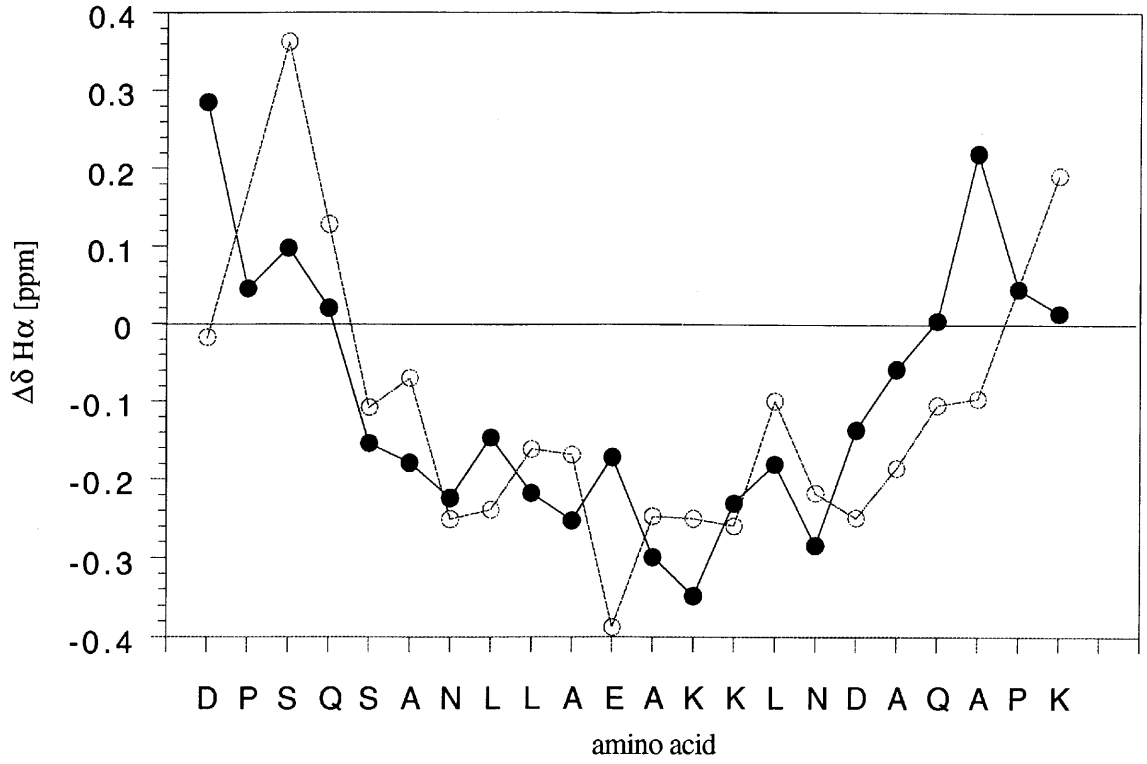

Figure 7 Effect of HFIP upon the conformational sensitive H^{α} chemical shifts of Ln (○) and Lr (●). Lr is shown from the carboxy to the amino terminus for comparison reasons.

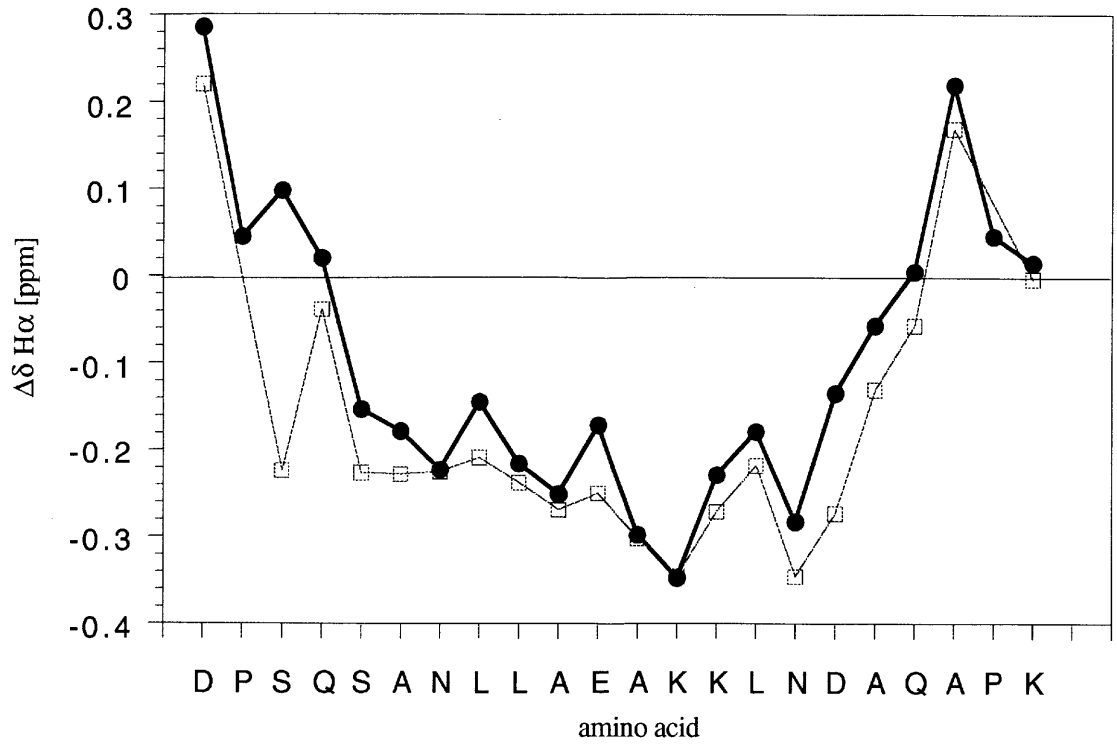

Figure 8 Differences of Ln H^{α} chemical shifts between 50% TFE (circles) and 18% HFIP (squares) at 5°C, pH = 5.3.

In general, CD and NMR studies showed in water a nascent helix for both Ln and Lr, throughout the sequence from Gln41 to Gln56. These nascent helices were clearly stabilized upon addition of cosolvents and specified as an amphiphilic helix, shown by CD and NMR. The close relation of 18% HFIP and 50% TFE for several conformationally sensitive NMR parameters such as NOEs and chemical shift deviation, in both absolute helical content and location of the helix, suggests a similar mechanism for helix stabilization upon addition of these fluorinated cosolvents. Earlier studies suggested that the differential solvation effect depends upon the highly hydrophilic nature of the peptide backbone [38], theoretical [39]). Thus, the use of mixed solvents should satisfy the optimal balance between electrostatic effects (favoured in organic solvents) and hydrophobic effects (favoured in water). A recent study from Kemp and coworkers [18] suggested destabilization of the unfolded state as the major driving force for the stabilization of nascent structure at low percentages of TFE. Thus, HFIP as cosolvent seems to disfavour the unfolded state more strongly than TFE, therefore inducing enhanced helicity.

The high helicity in fluorinated cosolvents was expected for the native peptide. Ln but was somewhat unexpected for the retro peptide Lr. Helix stability is normally viewed as the sum of different internal, or sequence-dependent, factors listed below (recently reviewed by Chakrabartty and Baldwin [6]) together with external factors such as temperature, solvent, pH, salt composition and concentration. The sequence-dependent factors are the intrinsic tendencies of amino acids to adopt a helical conformation and to form an N-terminal capping motif, side-chain backbone and side-chain to side-chain interactions such as salt-bridge formation, $\pi\pi$-stacking of aromatic residues or hydrophobic stabilization by residues spaced by $i,i+3$ or $i,i+4$ and, finally, charge–helix dipole interactions.

Comparative conformational analysis of different peptide sequences has been very useful in the identification of the stabilizing helical factors mentioned above. However, by this approach it is in general very difficult to weight the relative importance of each of these factors, especially because of the fact that the intrinsic tendency of each residue to adopt a helical conformation is, frequently, the dominant factor in the entire process. We think that a comparison of the conformation of a normal and a retro sequence represents a general approach to circumvent this problem, because both peptides contain the same residues in the same order but in a different orientation with respect to the macro dipole; thus, the sum of the intrinsic tendencies of each amino acid to adopt a helical conformation is identical in both peptides. In addition, in our particular case, the postulated salt-bridges exist for both Ln and Lr, one in a favoured (Ln Glu48–K51 and Lr K51–Asp54) and the other in an unfavoured (Lr Glu48–K51 and Ln K51–Asp54) orientation with respect to the macro dipole, thus contributing identically to the total helical amount. Nevertheless, strong differences occurred at the N- and C-termini. Whereas Asp38, in Ln, represents a good N-terminal helix capping motif, Lys59, in Lr, is considered to be a poor N-cap. The same residues contribute as well to the charge–macrodipole term in an opposite way. The negatively charges Asp38 interacts favourably with the partial positive amino terminus in Ln and unfavourably with the partial negative carboxy terminus in Lr, whereas the positively charged Lys59 interacts favourably with the partial negative carboxy terminus in Ln, and unfavourably with the N-terminus in Lr. In summary, it was expected that Ln would show much higher helicity than Lr, especially in the presence of non-polar solvents, such as 18% HFIP or 50% TFE, enhancing the ionic interactions as charge–macrodipole once. This general trend was confirmed quantitatively by CD measurements and on a residue basis applying the AGADIR [36] algorithm, which shows a higher total helicity for Ln than for Lr in water. However, the NMR results show equal helicity for Ln and Lr in both helical content and location of the helix on the sequence, despite the unfavourable interactions in Lr. These results strongly suggest that, among the different factors that govern the tendency of a given peptide sequence to adopt a helical conformation, N-capping and charge–marcodipole interactions are not the determinants of the tendency of the present peptide derived from the third helix of SpA DB to adopt a helical conformation. For this particular peptide it seems to be clear that helicity derives mostly from the appropriate side-chain interactions, especially from charge or hydrogen bond interactions of the amino acid pairs Glu48–Lys51 and Lys51–Asp54, both in $i,i+3$ spacing.

In conclusion, retro peptides and their normal counterparts can serve as conformational tools to discriminate between orientation dependent, such as capping for helices, and orientation independent, such as intrinsic helicity of each amino acid, secondary structure stabilizing factors.

ACKNOWLEDGEMENTS

We thank Dr P. Lloyd-Williams for careful reading and correction of the paper. Work at the University of Barcelona was supported by DGICYT (grant PB95-1131) and by the Generalitat de Catalunya (Centre de Referència en Biotecnologia and Grup Consolidat). This work has been carried out using the NMR facilities of the Serveis Científics I Tècnics of the University of Barcelona.

REFERENCES

1. M. M. Schemyakin, Y. A. Ovchinnikov and V. T. Ivanov (1969). Topochemical investigations on peptide systems. *Angew. Chem. Int. Ed. Engl 8*, 492–499.
2. V. Prelog and V. Gerlach (1964). Cycloenantiomerie und cyclodiastereomerie. *Helv. Chim. Acta 47*, 2288–2302.
3. M. Chorev and M. Goodman (1995). Recent developments in retro peptides and proteins–an ongoing topochemical exploration. *Trends Biotchnol. 13*, 438–445.
4. Y. M. Sánchez, T. Haack, M. J. Gonzalez, D. Ludevid and E. Giralt in: *Peptides 1995: Chemistry, Structure and Biology, Proceedings of the 14th American Peptide Symposium*, P. T. P. Kayumaya and R. S. Hodges, Eds., p. 558–560, Maryflower 1995.
5. G. Guichard, S. Muller, M. van Regenmortel, J. P. Briand, P. Mascagni and E. Giralt (1996). Structural limitations to antigenic mimicry achievable with retro-inverso (all-D-retro) peptides. *Trends Biotechnol. 14*, 44–45.
6. A. Chakrabartty and R. L. Baldwin (1995). Stability of alpha-helices. *Adv. Protein Chem. 46*, 141–176.
7. J. Deisenhofer (1981). Crystallographic refinement and atomic model of a human Fc fragment and its complex with fragment B of protein A from *Staphylococcus aureus* at 2.9 and 2.8Å resolution. *Biochemistry 20*, 2361–2370.
8. H. Gouda, H. Torigoe, A. Saito, M. Sato, Y. Arata and I. Shimana (1992). Three dimensional solution structure of the B domain of *Staphyloccocus aureus* protein A: Comparison of the solution and crystal structure. *Biochemistry 31*, 9665–9672.
9. M. Rance, O. W. Sørensen, G. Bodenhausen, G. Wagner, R. R. Ernst and K. Wüthrich (1983). Improved spectral resolution in COSY proton NMR spectra of proteins via double quantum filtering. *Biochem. Biophys. Res. Commun. 117*, 479–485.
10. C. Griesinger, G. Otting, K. Wüthrich and R. R. Ernst (1988). Clean TOCSY for ^{1}H spin system identification in macro molecules. *J. Am. Chem. Soc. 110*, 7870–7872.
11. A. Bax and D. G. Davis (1985). MLEV-17 based two dimensional homonuclear magnetic transfer spectroscopy. *J. Magn. Res. 65*, 355–360.
12. J. Jeener, B. H. Meier, P. Bachman and R. R. Ernst (1979). Investigation of exchange processes by two-dimensional NMR spectroscopy. *J. Chem. Phys. 71*, 4546–4553.
13. A. Kumar, R. R. Ernst and K. Wüthrich (1980). A two dimensional nuclear overhauser enhancement (2D NOE) experiment for the elucidation of complete proton-proton cross relaxation. *Biochem. Biophys. Res. Commun. 95*, 1–6.
14. A. A. Brother-Ny, R. L. Stephens, J. M. Lee, C. D. Warren and R. W. Jeanloz (1984). Structure determination of a tetrasaccharide: transient nuclear Overhauser effects in the rotating frame. *J. Am. Chem. Soc. 106*, 811–813.
15. M. Piorro, V. Saudek and V. Sklenár (1992). Gradient-tailored excitation for single-quantum NMR spectroscopy of aqueous solutions. *J. Biomol. NMRJ 2*, 661–665.
16. M. Goodman, A. S. Verdini, C. Toniolo, W. D. Philips and F. A Bovey (1969). Sensitive criteria for the critical size for helix formation in oligopeptides. *Proc. Natl Acad. Sci. USA 64*, 444–450.
17. F. D. Sönnichsen, J. E. V. Eyk, R. S. Hodges and B. D. Sykes (1992). Effect of trifluoroethanol on protein secondary structure: an nmr and cd study using a synthetic actin peptide. *Biochemistry 31*, 8790–8798.
18. A. Cammers-Goodwin, T. J. Allen, S. L. Oslick, K. F. McClure, J. H. Lee and D. S. Kemp (1996). Mechanism of stabilization of helical conformations of polypeptides by water containing trifluoroethanol. *J. Am. Chem. Soc. 188*, 3082–3090.
19. W. C. Johnson (1988). Secondary structure of proteins through circular dichroism spectroscopy. *Ann. Rev. Biophys. 17*, 145–166.
20. J. T. Yand, C. -S. C. Wu and H. M. Martínez (1986). Calculation of protein conformation from circular dichroism. *Methods Enzymol. 130*, 208–269.
21. P. E. Wright, H. J. Dyson and R. A. Lernet (1988). Conformation of peptide fragments of proteins in aqueous solution: Implications for initiation of protein folding. *Biochemistry 27*, 7167–7175.
22. K. Wüthrich: *NMR of Proteins and Nucleic Acids*. John Wiley & Sons, New York 1986.
23. H. J. Dyson, M. Rance, R. A. Houghten, R. A. Lerner and P. E. Wright (1988). Folding of immunogenic peptide fragments of proteins in water solution II: The nascent helix. *J. Mol. Biol. 201*, 201–217.
24. J. Rizo, F. J. Blanco, B. Kobe, M. Bruch and L. M. Gierasch (1993). Conformational behaviour of *Escherichia coli* OmpA signal peptides in membrane mimetic environments. *Biochemistry 32*, 4881–4894.
25. D. S. Wishart and B. D. Sykes (1994). Chemical shifts as a tool for structure determination. *Methods Enzymol. 239*, 363–392.

26. H. J. Dyson, M. Rance, R. A. Houghton and P. E. Wright (1988). Folding of immunogenic peptide fragments of proteins in water solution I. Sequence requirements for the formation of a reverse turn. *J. Mol. Biol. 226*, 161–200.
27. A. Bundi and K. Wüthrich (1979). Use of amide ^{1}H-NMR titration shifts for studies of polypeptide conformation. *Biopolymers 18*, 299–311.
28. K. D. Kopple, M. Ohnishi and A. Go (1969). Conformation of cyclic peptides III. Cyclopentaglycyltyrosyl and related compounds. *J. Am. Chem. Soc. 91*, 4264–4272.
29. M. Ohnishi and D. W. Urry (1969). Temperature dependence of amide proton chemical shift: The secondary structures of gramicidin S and Valinomycin. *Biochem. Biophys. Res. Commun. 36*, 194–202.
30. M. Eberstadt, G. Gemmecker, D. F. Mierke and H. Kessler (1995). Scalar coupling constants–their analysis and their application for the elucidation of structures. *Angew. Chem. Int. Ed. Engl. 34*, 1671–1695.
31. D. A. Case, J. Dyson and P. E. Wright (1994). Use of chemical shifts and coupling constants in nuclear and magnetic resonance structural studies on peptides and proteins. *Methods Enzymol. 239*, 392–416.
32. G. Merutka, H. J. Dyson and P. E. Wright (1995). 'Random Coil' ^{1}H chemical shifts obtained as a function of temperature and trifluoroethanol concentration for the peptide series GGXGG. *J. Biomol. NMR 5*, 14–24.
33. B. Odaert, F. Baleux, T. Huynhdinh, J. M. Neumann and A. Sanson (1995). Nonnative capping structure initiates helix folding in an Annexin-I fragment – a H-1-NMR conformational study. *Biochemistry 34*, 12820–12829.
34. V. Munoz and L. Serrano (1994). Elucidating the folding problem of helical peptides using empirical parameters. *Nature Struct. Biol. 1*, 399–409.
35. V. Munoz and L. Serrano (1995). Elucidating the folding problem of helical peptides using empirical parameters: II. Helix macrodipole effects and rational modification of the helical content of natural peptides. *J. Mol. Biol. 245*, 275–296.
36. V. Munoz and L. Serrano (1995). Elucidating the folding problem of helical peptides using empirical parameters: III. Temperature and pH dependence. *J. Mol. Biol. 245*, 297–308.
37. M. A. Jiminéz, M. Bruix;, C. Gonzáles, F. J. Blanco, J. L. Nieto, J. Herranz and M. Rico (1993). CD and ^{1}H-NMR studies of the conformational properties of peptide fragments from the C-terminal domain of thermolysin. *Eur. J. Biochem. 211*, 569581.
38. Nozaki and Tanford (1971). The solubility of amino acids and two glycine peptides in aqueous ethanol and dioxane solutions. *J. Biol. Chem. 246*, 2211–2217.
39. Brooks and Nielsen (1993). Promotion of helix formation in peptides dissolved in alcohol and water–alcohol mixtures. *J. Am. Chem. Soc. 115*, 11034–11035.

